Noninvasive blood glucose detection using a miniature wearable Raman spectroscopy system

Yi Zheng (郑 毅)[1,2], Xiangping Zhu (朱香平)[1], Zhe Wang (王 哲)[3], Zongyu Hou (侯宗余)[3], Fei Gao (高 飞)[1], Rongzhi Nie (聂荣志)[1,4], Xiaoxia Cui (崔晓霞)[1], Jiangbo She (佘江波)[1], and Bo Peng (彭 波)[1,*]

[1]*State Key Laboratory of Transient Optics and Photonics, Xi'an Institute of Optics and Precision Mechanics, Chinese Academy of Science (CAS), Xi'an 710119, China*

[2]*University of Chinese Academy of Sciences (CAS), Beijing 100049, China*

[3]*State Key Laboratory of Power Systems, Department of Thermal Engineering, Tsinghua-BP Clean Energy Center, Tsinghua University, Beijing 100084, China*

[4]*School of Science, Xi'an Jiaotong University, Xi'an 710049, China*

**Corresponding author: bpeng@opt.ac.cn*

Received February 22, 2017; accepted May 18, 2017; posted online June 16, 2017

In this Letter, a miniature wearable Raman spectroscopy system is developed. A wearable fiber-optic probe is employed to help the stable and convenient collection of Raman spectra. A nonlinear partial least squares model based on a multivariate dominant factor is employed to predict the glucose level. The mean coefficients of determination are 0.99, 0.893, and 0.844 for the glucose solution, laboratory rats, and human volunteers. The results demonstrate that a miniature wearable Raman spectroscopy system is feasible to achieve the noninvasive detection of human blood glucose and has important clinical application value in disease diagnosis.

OCIS codes: 300.6450, 300.6190, 120.4290, 170.1470.
doi: 10.3788/COL201715.083001.

Nowadays, there are about 415 million adults suffering from diabetes[1]. At present, the treatment for diabetes patients is monitoring their blood glucose level frequently and then taking the appropriate amount of oral hypoglycemic drugs and insulin to control their blood glucose level. Since conventional methods of blood sampling are painful, discontinuous, and have other undesirable features, noninvasive methods are attractive for monitoring blood glucose as well as other analytes[2].

Various methods, such as Raman spectroscopy[3–14], near-infrared spectroscopy[15,16], photo-acoustic spectroscopy[17,18], and optical coherence tomography[19,20], have been extensively researched. Raman spectroscopy displays excellent molecular specificity by probing the fundamental vibrational states. Due to the extremely weak Raman scattering signal of water, sharper spectral features, and few spectral overlaps, Raman spectroscopy is particularly suitable for detecting biological analytes.

However, conventional laboratory Raman systems, with their large size, cumbersome nature, and high cost, are limited in clinical applications. Additionally, the stability is not good enough. Conventional Raman detection systems always utilize a convex lens with a certain focal length as the collecting lens, but the focal position will change during the measurement. The problem that Raman signal cannot be stably collected will greatly affect the accuracy and stability of the test.

In this Letter, a thallium-doped grin lens was employed as the collection lens. A specially designed wearable fiber-optic probe was employed to help the stable and convenient collection of the Raman spectrum. A novel method of quantitative analysis of the Raman spectrum that uses the peak area as the main reference factor and the peak intensity as the auxiliary reference factor to calculate the target concentration was proposed. A nonlinearized multivariate dominant factor-based partial least squares (PLS) model was employed for different samples to predict the glucose levels. A glucose solution, 11 rats, and 10 healthy humans were studied as the subjects.

Figure 1 shows the experimental setup. According to the investigation by Enejder[3,4], a 785 nm diode laser (B&Wtek, BRM-OEM-785-0.3-100-0.22-FC) with a

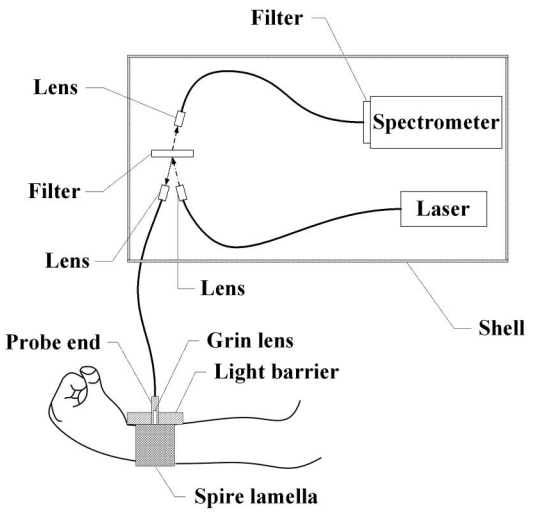

Fig. 1. Experimental setup: the schematic diagram of the miniature wearable Raman spectroscopy system.

stable power of 300 mW and a linewidth of 0.2 nm was employed as the excitation source and could ensure the harmlessness and high efficiency of the detection system.

A specially designed wearable fiber-optic probe was employed. The probe end packaged the grin lens, while a shading tube was designed to reduce the interference of ambient light and to help fasten the probe with a spire lamella. This probe utilized a thallium-doped grin lens as the collecting lens, which could ensure that the focal position is always on the surface of the measured object while realizing the convergence of wide-band spectra. Only one kind of filter (Semrock, LP02-785RU-25), which could reflect the light below 785 nm while transmitting the light between 805 and 1050 nm, was used in this probe. The function of this filter amounted to the function of a dichroic mirror and a bandpass filter.

Compared with a conventional probe, this probe had the advantages of better testing stability and lower cost and is convenient to wear.

A miniature Raman spectrometer (B&Wtek, BTC675 N-OEM), with dimensions of 124 mm × 92 mm × 26 mm, an optical resolution of 6 cm^{-1} and a signal-to-noise ratio (SNR) of 4800:1, was employed to detect the Raman spectroscopy. The external optical system was a Czerny–Turner system. A back-illuminated linear-array CCD (Hamamatsu Photonics, S11156-2048-01), with 2048×1 pixels, was selected as the detector. A thermoelectrically cooled module, with a cooler temperature of 50°C below the ambient temperature, was employed to reduce the dark noise while increasing the SNR and sensitivity of the detection system.

All of the components were immobilized compactly to achieve the miniaturization of this system.

Glucose solutions which aimed to reflect the blood glucose levels of humans (4.4–11.1 mmol/L) were prepared, with different concentrations of 3.8, 4.1, 4.4, 4.8, 5.1, 5.4, 5.6, 6.7, 7.8, 8.9, 10, 11.1, 12.2, and 13.3 mmol/L. A cuvette containing the glucose solution was put into a dark sample cup to ensure the stabilization of the test. Raman spectra were collected after 20 s. The glucose solution study was employed for verifying the feasibility of in vitro glucose detection using the miniature wearable Raman system.

Eleven Sprague–Dawley (SD) male rats were studied as samples. We here claim that our protocol was approved by XIOPM's committee on the use of SD rats and human volunteers as experimental subjects. After fasting for 8 h, the rats were anesthetized. Then, the glucose solution was poured into the stomachs of rats. As a result, the blood glucose levels of the rats varied within 1.5 h. Raman spectra were collected transcutaneously every 5 min from the ears of the rats along with glucose reference values provided by a blood glucose meter (Roche, ACCU-CHEK, Active). The laboratory rat study was employed for verifying the feasibility of noninvasive detection of an in vivo blood glucose level using the miniature wearable Raman system.

Ten human volunteers were investigated as samples. Volunteers took a certain dose (2 g/kg) of glucose solution orally. During the next 2 h, Raman spectra were collected transcutaneously every 20 min from the inside of the wrist while glucose reference values were provided by a blood glucose meter. Every volunteer was tested at least 3 times to ensure the repeatability of the experiment. The skin of the human volunteers was not damaged during the test. The human subject study was employed for verifying the feasibility of noninvasive detection of human blood glucose level using the miniature wearable Raman system.

The area of characteristic peaks was used mainly as a calibration reference, while the intensity was used as an auxiliary calibration reference to avoid the interference of baseline fluctuations of Raman spectra. Raman spectra were extracted at the range of 300–3000 cm^{-1} without any pre-processing to avoid errors.

A dominant factor-based multivariate PLS model was employed to predict the glucose concentration[21–23]. The dominant factor could model the linear and nonlinear relationships according to the physical background, while a statistical-based PLS method was used thereafter to correct the residue errors using the full spectral information. The R^2 value and mean absolute error (MAE) are the two indexes used to estimate the fitted result. A higher R^2 value and lower MAE mean a better fitted result. The basic principle of the model can be written as

$$Y = f(x) + E_1, \tag{1}$$

where Y is the glucose level, $f(x)$ is the dominant factor, and E_1 is the residue error.

$$\begin{aligned} f(x) = {} & k_1 x_1 + k_2 x_2 + \cdots + k_n x_n \\ & + k_{n+1} x_1^2 + k_{n+2} x_2^2 + \cdots + k_{2n} x_n^2 + b, \end{aligned} \tag{2}$$

where x is the area of the characteristic peaks whose position is similar to the characteristic peaks of the Raman spectrum of glucose. $k_1, k_2, ..., k_{2n}$ could be calculated by the PLS.

$$Y_2 = g(x) + E_2, \tag{3}$$

$$\begin{aligned} g(x) = {} & j_1 x_1 + j_2 x_2 + \cdots + j_m x_m \\ & + j_{m+1} x_1^2 + j_{m+2} x_2^2 + \cdots + j_{2m} x_m^2 + c, \end{aligned} \tag{4}$$

where x is the intensity of the characteristic peaks whose position is different from the characteristic peaks of the Raman spectrum of glucose. $j_1, j_2, ..., j_{2m}$ could be calculated by the PLS.

$$R^2 = \frac{S_1}{S_2} = 1 - \frac{S_3}{S_2} = 1 - \frac{\sum_{i=1}^{n} (y_i - \hat{y}_i)^2}{\sum_{i=1}^{n} (y_i - \bar{y})^2}, \tag{5}$$

where S_1 is the regression sum of squares, S_2 is the total sum of squares, and S_3 is the residual sum of squares.

$$\mathrm{MAE} = \frac{1}{n}\sum_{i=1}^{n}|f_i - Y_i|, \tag{6}$$

where f_i is the calculated value, while Y_i is the measured value.

Figure 2 exhibits the Raman spectra of the glucose solution. The signal at 1372.7 cm^{-1}, which was considered as the CH_{3-} of glucose, is the strongest. According to Fig. 3, the relationship between the intensity of 1372.7 cm^{-1} and the concentration of glucose is uncorrelated. However, the area of 1372.7 cm^{-1} and the concentration of glucose are directly related. Consequently, the areas of peaks were employed as the main reference of calculation. The calibration result shown in Fig. 4 with the MAE is 0.394 mmol/L, and the R^2 value is 0.981, which encourages us to do further research.

Figure 5 exhibits the difference between the spectrum of the skin of a rat and the glucose solution. It can be seen that the skin of a rat has similar characteristic peaks with glucose at 406, 502, 586, 670, 767, 1200, 1256, 1447, 1555, and 1656 cm^{-1}. Figure 6 shows the predicted blood glucose levels for one of the rat samples using leave-one-out cross validation to confirm the best value of the principal component. The calculated results of the R^2 values are 0.954, 0.953, 0.952, and 0.951, showing the

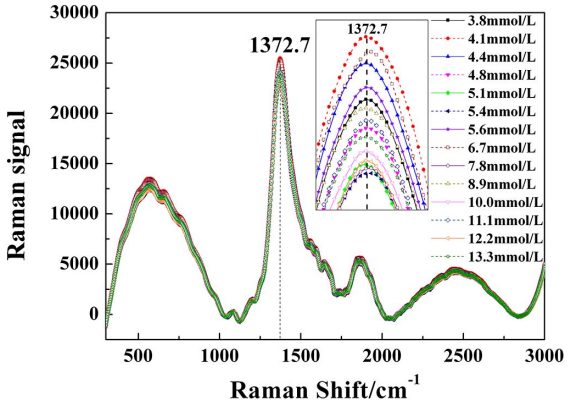

Fig. 2. (Color online) Raman spectra of glucose solutions with concentrations of 3.8–13.3 mmol/L. The area of 1372.7 cm^{-1} and the concentration of glucose are directly related.

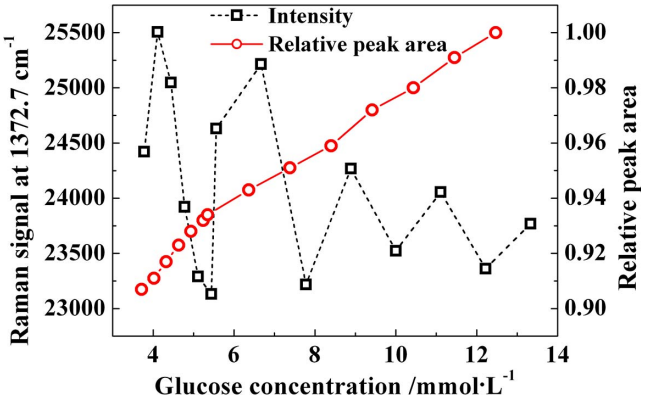

Fig. 3. (Color online) Difference between the relationship of the peak area and intensity with the concentration of the glucose solution.

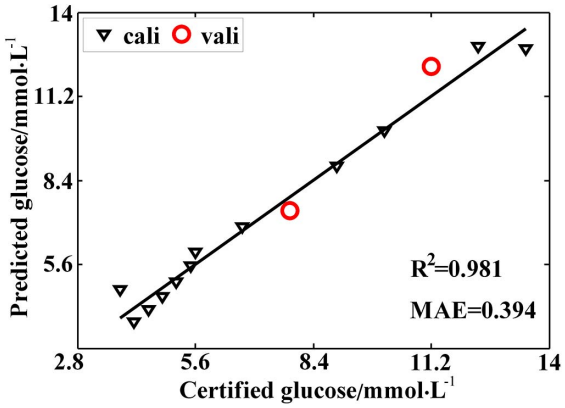

Fig. 4. (Color online) Calculated result of the glucose solution, with a coefficient of determination of 98.1% and an MAE of 0.394 mmol/L.

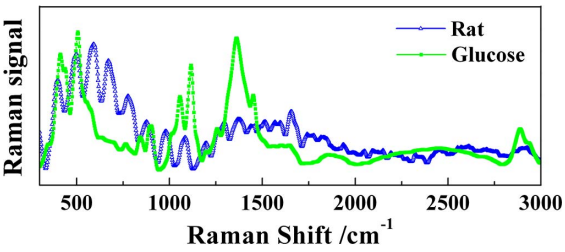

Fig. 5. (Color online) Comparison between the spectrum of the rat skin and the spectrum of the glucose solution. The spectrum of the rat skin is more complicated.

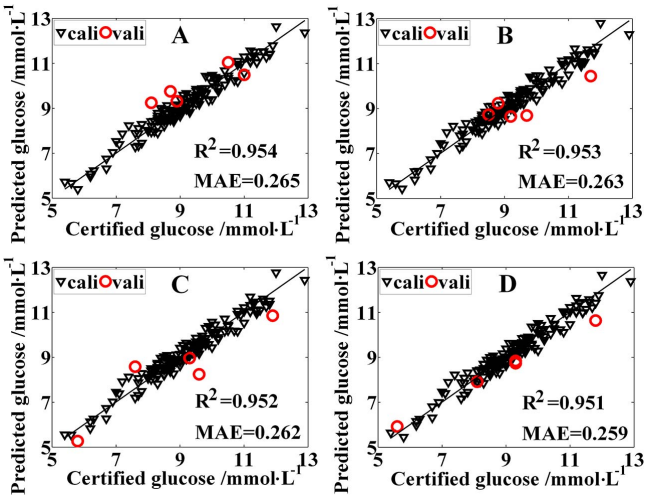

Fig. 6. (Color online) Calculated results for one of the rat samples.

Table 1. Summary of Results from Cross-Validated Calibrations Generated from Data Set of Measurements on Each of the 11 Laboratory Rats

Rat	R^2	MAE (mmol/L)	Sample Capacity
1	0.960	0.149	25
2	0.954	0.265	147
3	0.924	0.543	53
4	0.905	0.310	77
5	0.893	0.279	53
6	0.889	0.130	23
7	0.879	0.227	24
8	0.868	0.184	23
9	0.853	0.159	30
10	0.851	0.217	229
11	0.851	0.306	51
Mean	0.893	0.252	67

accuracy and stability of the calibration model and this miniature wearable Raman system.

Each sample was processed individually in the same method, and the results are shown in Table 1. The mean R^2 value for all 11 rats is 0.893, while all of the rat samples have R^2 values over 0.85. The results suggest that this miniature wearable Raman system is feasible for in vivo blood glucose detection.

Figure 7 shows the comparison of the Raman spectrum of human skin with those of the glucose and rat. The

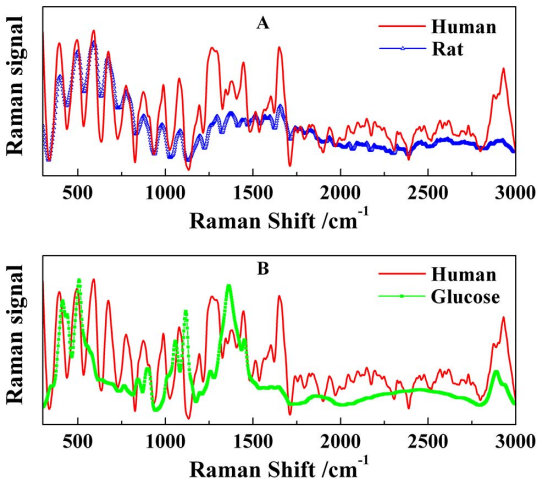

Fig. 7. (Color online) (A) Comparison between the spectrum of the human skin and the spectrum of the rat skin. (B) Comparison between the spectrum of the human skin and the spectrum of glucose. The spectrum of the human skin is similar to the spectrum of the rat skin.

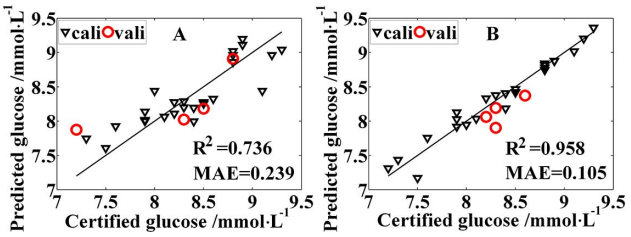

Fig. 8. (A) Calculated result for one of the human volunteers without using a grin lens. (B) Calculated result for one of the human volunteers using a grin lens. The result when using a grin lens is obviously better.

Raman spectra of human skin were extremely similar to the spectra of rat skin.

Figure 8 shows the calculated results with and without the grin lens for one of the human volunteers. The R^2 value is 0.958 with the grin lens, while the R^2 value is 0.736 without the grin lens. The result shows that using the grin lens is of great significance to the accuracy and stability of the test.

The results for all of the human volunteers are shown in Table 2. The mean R^2 value for all 10 volunteers is 0.844. The results suggest that this miniature wearable Raman system is feasible for human blood glucose detection.

Figures 9(A) and 9(B) exhibit the predicted results for all of the rat samples with an R^2 of 0.563, while one of the rat samples has an R^2 of 0.960. Figures 9(C) and 9(D) exhibit the predicted results for all of the human volunteers with an R^2 of 0.773, while one of the human volunteers has an R^2 of 0.935. The result corroborates that modeling for each sample is essential to ensure the purity and accuracy of the calculation.

The reasons for these results may come from two aspects: individual differences and physiological changes.

Table 2. Summary of Results from Cross-Validated Calibrations Generated from Data Set of Measurements on Each of the 10 Human Volunteers

Human	R^2	MAE (mmol/L)	Sample Capacity
1	0.958	0.105	29
2	0.935	0.379	59
3	0.866	0.285	21
4	0.85	0.275	37
5	0.835	0.398	35
6	0.83	0.407	37
7	0.827	0.620	35
8	0.815	0.317	35
9	0.765	0.455	35
10	0.759	0.410	21
Mean	0.844	0.365	34

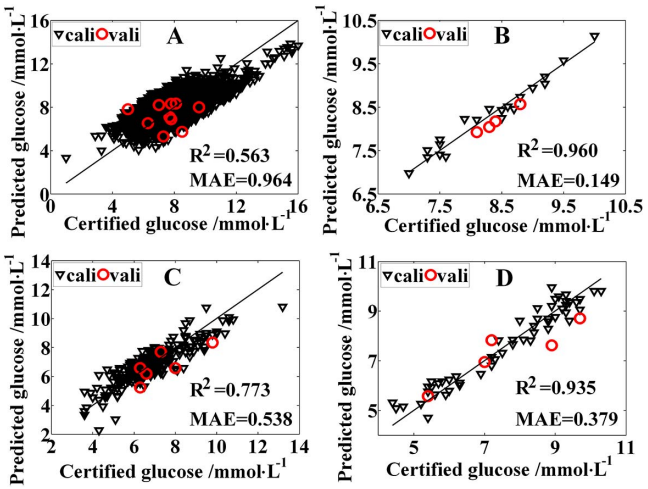

Fig. 9. (Color online) Comparison between calculated results for all samples and one of the samples.

However, we anticipate that the more accurate result can be predicted by the methods of big data statistics and establishing a glucose database.

In conclusion, signal acquisition and data analysis are the 2 major bottlenecks of noninvasive blood glucose detection. In this Letter, a novel method of Raman spectra collection is investigated. A thallium-doped grin lens is employed as the collection lens. A specially designed wearable fiber-optic probe is employed to help the stable and convenient collection of the Raman spectrum. A miniature wearable Raman system is developed to achieve the noninvasive blood glucose detection. The area of characteristic peaks is used as the main calibration reference, while the intensity is used as the auxiliary calibration reference. Additionally, a dominant factor-based multivariate PLS model is constructed to achieve the accurate prediction of blood glucose levels. This serious study investigates *in vitro* and *in vivo* glucose detection using a miniature wearable Raman spectroscopy system and demonstrates the feasibility of noninvasive blood glucose detection using this miniature wearable Raman spectroscopy system. The results may be useful for the development of a miniature Raman spectrometer in disease diagnosis and clinical applications of blood glucose as well as other analyte detection.

This work was supported by the National Natural Science Foundation of China (NSFC) under Grant No. 61308086. We would like to thank the researchers from the Fourth Military Medical University for raising the rats and for the valuable suggestions.

References

1. J. D. R. Fernandes, K. Ogurtsova, U. Linnenkamp, L. Guariguata, T. Seuring, P. Zhang, D. Cavan, and L. E. Makaroff, Diabetes Res. Clin. Pract. **117**, 48 (2016).
2. D. C. Klonoff, Diabetes Care **20**, 433 (1997).
3. A. M. K. Enejder, T. G. Scecina, J. Oh, M. Hunter, W. C. Shih, S. Sasic, G. L. Horowitz, and M. S. Feld, J. Biomed. Opt. **10**, 031114 (2005).
4. A. M. K. Enejder, T. W. Koo, J. Oh, M. Hunter, S. Sasic, M. S. Feld, and G. Horowitz, Opt. Lett. **27**, 2004 (2002).
5. N. C. Dingari, I. Barman, G. P. Singh, J. W. Kang, R. R. Dasari, and M. S. Feld, Anal. Bioanal. Chem. **400**, 2871 (2011).
6. W. C. Shih, K. L. Bechtel, and M. V. Rebec, J. Biomed. Opt. **20**, 051036 (2015).
7. W. C. Shih, K. L. Bechtel, and M. S. Feld, Opt. Express. **16**, 12726 (2008).
8. K. L. Bechtel, W. C. Shih, and M. S. Feld, Opt. Express **16**, 12737 (2008).
9. A. J. Berger, I. Itzkan, and M. S. Feld, Spectrochim. Acta A Mol. Biomol. Spectrosc. **53A**, 287 (1997).
10. A. J. Berger, T. W. Koo, I. Itzkan, G. Horowitz, and M. S. Feld, Appl. Opt. **38**, 2916 (1999).
11. D. A. Stuart, J. M. Yuen, N. C. Shah, O. Lyandres, C. R. Yonzon, M. R. Glucksberg, J. T. Walsh, and R. P. Van Duyne, Anal. Chem. **78**, 7211 (2006).
12. Z. Yan, C. Li, L. Yang, J. Zhao, H. Yang, P. Verma, and S. Kawata, Chin. Opt. Lett. **13**, 102401 (2015).
13. X. Tan, L. Jiang, J. Hu, P. Liu, A. Wang, and Y. Lu, Chin. Opt. Lett. **13**, 111401 (2015).
14. A. Z. Subramanian, E. Ryckeboer, A. Dhakal, F. Peyskens, A. Malik, B. Kuyken, H. Zhao, S. Pathak, A. Ruocco, A. D. Groote, P. Wuytens, D. Martens, F. Leo, W. Xie, U. D. Dave, M. Muneeb, P. V. Dorpe, J. V. Campenhout, W. Bogaerts, P. Bienstman, N. L. Thomas, D. V. Thourhout, Z. Hens, G. Roelkens, and R. Baets, Photon. Res. **3**, B47 (2015).
15. S. F. Malin, T. L. Ruchti, T. B. Blank, S. N. Thennadil, and S. L. Monfre, Clin. Chem. **45**, 1651 (1999).
16. J. Liu, R. Liu, and K. Xu, Appl. Spectrosc. **69**, 1313 (2015).
17. H. A. Mackenzie, H. S. Ashton, S. Spiers, Y. Shen, S. S. Freeborn, J. Hannigan, J. Lindberg, and P. Rae, Clin. Chem. **45**, 1587 (1999).
18. R. Weiss, Y. Yegorchikov, A. Shusterman, and I. Raz, Diabetes Technol. Ther. **9**, 68 (2007).
19. L. Zhu, J. Lin, B. Lin, and H. Li, Chin. Opt. Lett. **11**, 021701 (2013).
20. M. G. Ghosn, V. V. Tuchin, and K. V. Larin, Opt. Lett. **31**, 2314 (2006).
21. J. Feng, Z. Wang, L. Z. Li, Z. Li, and W. D. Ni, Appl. Spectrosc. **67**, 291 (2013).
22. Z. Wang, J. Feng, L. Z. Li, W. D. Ni, and Z. Li, J. Anal. At. Spectrom. **26**, 2289 (2011).
23. J. Feng, Z. Wang, L. West, Z. Li, and W. D. Ni, Anal. Bioanal. Chem. **400**, 3261 (2011).